Measurement 45 (2012) 702–710

Contents lists available at SciVerse ScienceDirect

Measurement

journal homepage: www.elsevier.com/locate/measurement

# The investigation of the lower limb geometry using 3D sonography and magnetic resonance

Ewelina Świątek-Najwer [a,*], Krzysztof Krysztoforski [a], Szymon Łukasz Dragan [b], Romuald Będziński [a]

[a] Wrocław University of Technology, Division of Biomedical Engineering and Biomechanics, Łukasiewicza 7/9, 50-371 Wrocław, Poland
[b] Academic Hospital in Wroclaw, Orthopedics and Traumatology Clinic, Borowska Str. 213, 50-556 Wrocław, Poland

ARTICLE INFO

*Article history:*
Received 21 March 2011
Received in revised form 5 October 2011
Accepted 28 December 2011
Available online 8 January 2012

*Keywords:*
Biomedical engineering
Computer aided surgery
Free-hand sonography
Magnetic resonance imaging
Biomechanics

ABSTRACT

The main aim of this work was to test the developed system of a free hand sonographic probe in the clinical conditions. The measuring system consists of navigation system tracking the position of a linear ultrasound probe and the self-developed software to control the tools and analyse the recorded data. It enables both measurement of geometrical parameters according to the self-designed template and the identification of the three dimensional shape of bone. Moreover the software provides virtual planning of surgery and supports the surgeon to execute the planned scenario in the reality.

The paper describes the three methods of the ultrasound probe calibration and the obtained results of calibration affecting the accuracy of measurement.

There have been performed tests of the femur and tibia mechanical axes, the mechanical axis of the lower limb and the neck-shaft angle using 3D ultrasound imaging and magnetic resonance imaging, on a group of five probands. The results revealed high Pearson's correlation coefficient and small deviations estimated to 0.4–3.5 mm and 2°.

The 3D ultrasound tests of limb geometry were performed on seven patients suffering from limb deformities and three patients treated with Ilizarov External Fixator. The measurements enable planning and post-operative diagnosing of limb corrections with lengthening.

The results of measurements are analyzed in terms of applicability in clinical conditions.


## 1. Introduction

The aiding of the orthopedic surgery requires high resolution three dimensional imaging techniques in order to plan the surgical procedure and diagnose the disease such as bone deformation. Typically ordained Computed Tomography is an X-ray examination, introducing relevant radiation dose into the human body. The magnetic resonance imaging is an efficient, noninvasive, high contrast soft tissue imaging technique, however it is expensive and difficult to apply intraoperatively. The ultrasound imaging is a non-invasive technique to differentiate tissues by acoustic impedances.

Nowadays the sonography provides the high resolution imaging with the quality obtained in case of magnetic resonance imaging. It is the advantage of harmonic imaging with double basic frequency. The latest trends of development in ultrasound imaging are: the spatial imaging techniques and the integration of ultrasounds into monitoring of diagnostic and therapeutic methods, such as control of targeted drug delivery [9].

Mostly applied method of 3D ultrasound imaging in pregnancy and soft tissues diagnosing requires tilting of the ultrasonic beam controlled by precise electronic controls, mechanical engines, phase array and selection of working transmitters [8]. Three dimensional ultrasound

* Corresponding author.
*E-mail address:* ewelina.swiatek-najwer@pwr.wroc.pl (E. Świątek-najwer).

0263-2241/$ - see front matter © 2012 Elsevier Ltd. All rights reserved.
doi:10.1016/j.measurement.2011.12.020

imaging using mechanical scanning assemblies found application in breast biopsy and prostate therapy [1]. The free hand three dimensional ultrasound imaging applying the electromagnetic or optical navigation to control the position of ultrasound probe is currently developed in biomedical engineering [13].

The experience in sonography examination has a critical influence on the imaging quality, since the angle of the sound beam and the degree of tissues compression affects the ultrasound image. An important issue concerning the free hand sonography is also the accuracy of the ultrasound probe calibration. The aim of this procedure is to calculate the matrix transforming a point of ultrasound scan into the coordinate system of a sensor mounted on probe. The analysis of papers on ultrasound probe calibration showed that the main types of phantoms are: the network of markers (wires), the plane visualization, the so called "N" or "Z" wire-phantoms and the Cambridge phantom (with steel lines) [12].

The ultrasound systems have found application in musculoskeletal measurements. Keppler describes the tests of bone geometry using a free hand ultrasound system on patients before and after lower limb osteosynthesis [3]. The ultrasound imaging is also applied in the measurements of muscles physiological parameters, such as physiological cross-sectional area and the volume of muscles [16].

The US intra-operative imaging is nowadays applied as a method to register landmarks defining the patient coordinate system or parameters such as the mechanical limb axis during Total Hip Arthroplasty. Kiefer and Mainard stated that the ultrasound measurement is more precise than standard palpation performed using a navigated pointer, especially when the symphysis pubis is identified in case of obese patients [4,11].

The three dimensional ultrasound intra-operative imaging has also found an application in the neurosurgery. In SonoWand Invite system by Elekta Neuroscience, the navigated ultrasound probe provides rapid access to intra-operative 3-D images in high quality. The real-time imaging is crucial during minimally invasive neurosurgery. The system also applies the results of preoperative CT or MR imaging. A very useful feature is that the surgeon can observe any cross-sectional slice calculated from the pre-operative dataset according to the real-time position of ultrasound probe. Simultaneously the surgeon observes the intra-operative ultrasound image [14].

The ultrasound measurements using the developed 3D free hand system for orthopaedic surgery provides a valuable complement to the X-ray examinations. Ultrasound imaging is readily available in intra-operative conditions and useful for computer assisted surgical procedures to register characteristic points of the bone in the patient reference system. The ultrasound intraoperative imaging enables to follow the surgical scenario designed during the virtual planning using any 3D image data (ultrasound, CT, MRI). The ultrasound imaging helps to complete registration procedure. Basing on the collected characteristic points related to the patient coordinate system, the matching matrix is calculated and the virtual data are transformed to the intraoperative coordinate system. Through this procedure, the surgeon can track the position of any surgical instruments regarding all preoperative image-based virtual models of tissues. Moreover, the developed ultrasound system provides identification of the bone shape for virtual planning of surgical procedures and supporting the real time surgical procedures [15].

This paper describes the results of comparative tests of the lower limb geometry applying the developed ultrasound free hand system and magnetic resonance imaging (test performed for healthy probands). The 3D sonographic tests of seven patients suffering from limb deformities were performed to check the system in case of nonphysiological state. To check the usability of the developed tool in the most difficult conditions, three patients under osseointegration treatment (using Ilizarov External Fixator) were examined.

## 2. Materials and methods

A free-hand ultrasound measuring system combining the ultrasound machine EchoBlaster 128, (Telemed, Lithuania) and the optical tracking system Polaris Spectra (NDI, Canada) has been developed. It allows for control of the ultrasound probe position in a specified reference system. The idea of the system and the results of the tests in laboratory conditions have already been described in details in paper by Świątek-Najwer [15] (see Fig. 1).

### 2.1. Calibration phantom

To calibrate the ultrasound probe a new calibration phantom has been designed. Its construction differs from existing phantoms. The calibrating markers are made of wire with 0.5 mm diameter, which creates five levels of double "N" structures (see Fig. 2). The levels 1, 3, and 5 are identical and shaped as double "N" structures differing in the geometry, whereas the levels: 2 and 4 create double inversed "N" structures also differing in the geometry (Fig. 2).

To measure the locations of holes in the phantom the 3D-Real-Time-Motion-Capture System – Optotrak Certus (full focus e-type) (NDI, Canada) has been applied. Its accuracy in dynamic conditions is as high as 0.15 mm. However the measurements have been performed in static conditions, therefore the accuracy was higher. The deviation of

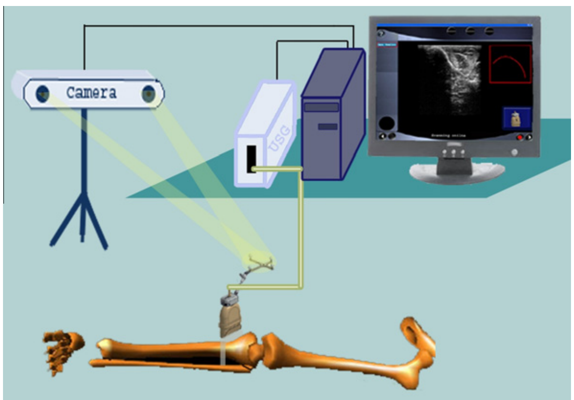


**Fig. 1.** A scheme of 3D sonography to investigate bone geometry.

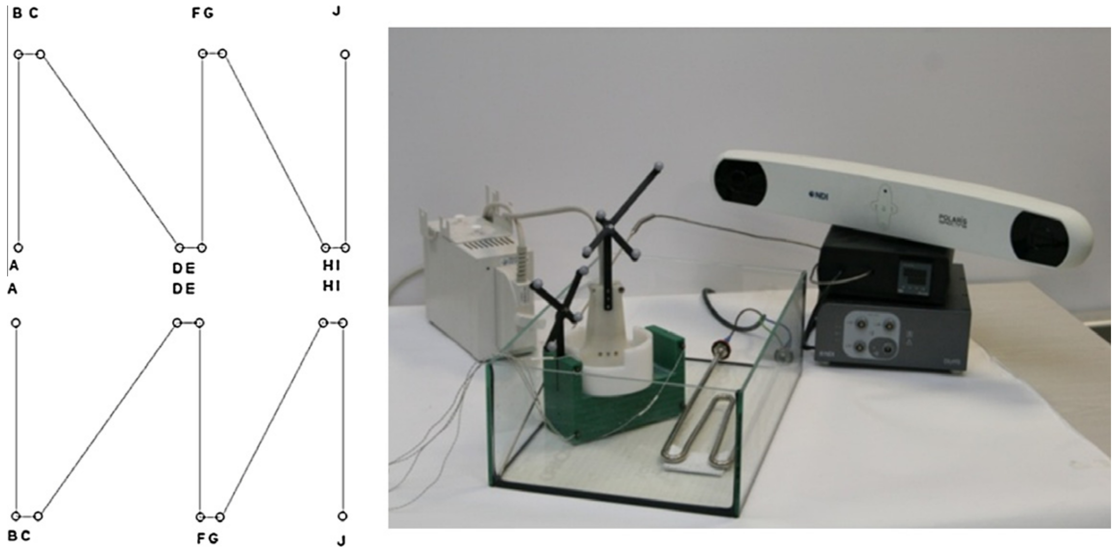


**Fig. 2.** The configuration of double "N" levels in the calibration phantom.

the measured coordinates was estimated to 0.0001 mm. A pointer with curled tip has been designed and produced to measure the locations of holes (Fig. 3). The positions of holes for wires mounting (A–J) in the phantom were related to the coordinate system defined by the reference frame mounted on phantom.

The second phantom construction contained eight metallic foveae mounted on the corners of the two square plates on different levels. The positions of the foveae have been measured with Zeiss coordinate machine. The main advantage of the phantom is that the foveae are easily identified on the ultrasound scan (see Fig. 4).

### 2.2. Methods of calibration

To calibrate the ultrasound probe, the wire phantom was immersed in the water with stabilized temperature at 37.0°, and the probe was introduced into the rim over the phantom to record scans (see Fig. 2). The ultrasound scans and the ultrasound probe locations (in the phantom reference coordinate system) were recorded simultaneously. On the ultrasound image the 25 echoes of the wires were identified manually (see Fig. 5) and the inter-echoes distances were measured taking into account the depth of scanning and the width of probe [7].

**Fig. 3.** A self-designed pointer to define the positions of holes in the calibration phantom.

Basing on the assertion of triangles similarity, the positions of fiducial echoes (in the reference coordinate system) were determined [5,6]. The transformation matrix from the image coordinate system to the phantom coordinate system is the product of the unknown calibration matrix and the transformation matrix from the phantom to the on-probe sensor coordinate system.

Two methods of calibration have been applied (also presented in [7]).

1. First method was to minimize the sum of distances between the proper echoes positions in the phantom reference frame coordinate system ($xP_i$, $yP_i$, $zP_i$) and the positions of the ultrasound echoes transformed by the unknown calibration matrix ($xF_i$, $yF_i$, $zF_i$).
2. The main idea of the second method was to calculate the calibration matrix basing on the fitted ultrasound scanning plane in space. To fit the least square orthogonal plane to the locations of 25 echoes, the Singular Value Decomposition was applied. To define the transformation matrix from the image coordinate system to the coordinate system of the phantom reference sensor, the position of the image coordinate system origin in the phantom coordinate system and the directional vectors of axes were defined. Finally the calibration matrix was calculated basing on linear matrix equation.

The third method of calibration applied the calibration plate with eight foveae. The echoes of foveae were identified on eight separate scans. The transformation matrix from the coordinate system of sensor mounted on probe to the coordinate system of the reference sensor mounted on the plate was recorded simultaneously with each scan. The calibration matrix was calculated to optimize the

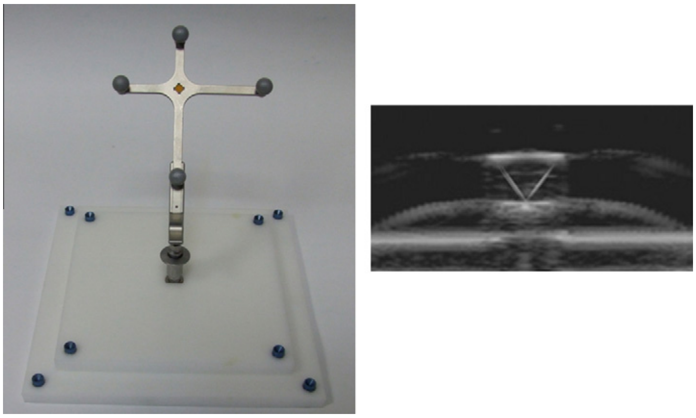

**Fig. 4.** The calibration plate and the ultrasound scan of a metallic fovea.

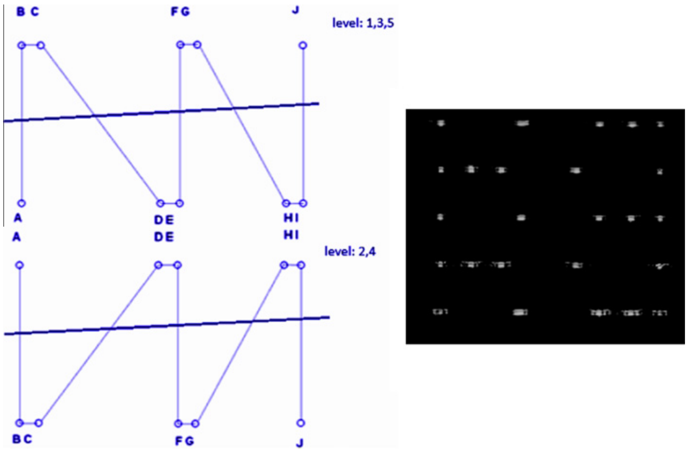


**Fig. 5.** An ultrasound image with echoes of wire fiducials.

distance between the calculated and the measured (by Zeiss coordinate machine) positions of the foveae in the coordinate system of sensor mounted on plate. The depth of scanning and the width of linear probe were taken into account.

### *2.3. Clinical tests of the developed system*

The purposes of clinical tests were as following:

1. A comparative analysis of the limb geometrical parameters investigated using the ultrasound system and the parameters measured on the magnetic resonance images (test performed for **probands**).
2. The tests of the limb geometrical parameters on the **patients suffering from limb deformities**.
3. The tests of limb geometrical parameters on the **patients, who undergo osteosynthesis applying the Ilizarov External Fixator**.

All these measurements were performed applying the dynamic reference frame (DRF) mounted noninvasively on the anterior surface of shank using a blood arrest band. The location of the DRF was selected because of its stable position on the shank. The DRF defines one anatomical coordinate system. The position of patient on the adapted couch is crucial. Since only one DRF is applied, the rotation and position of the shank in relation to the thigh need to be constant during the measurement. Therefore, the feet and the distal part of thigh were stabilized, also the patient was asked to lay still during the procedure. So far the tests applying two reference frames have been performed to identify landmarks of pelvis (anterior superior iliac spines and symphysis pubis). However, the tests revealed that one DRF is sufficient to identify landmarks of the lower limb to provide both repeatability and accuracy of the measurement.

All the ultrasound tests were performed by operator, whose level of experience in orthopaedic sonography is as high as 3 years. The total number of examined patients was 15: 5 healthy probands were examined using ultrasound and MRI, 7 patients experiencing limb deformity and 3 patients who undergo osteosynthesis applying Ilizarov External Fixator were examined using ultrasound.

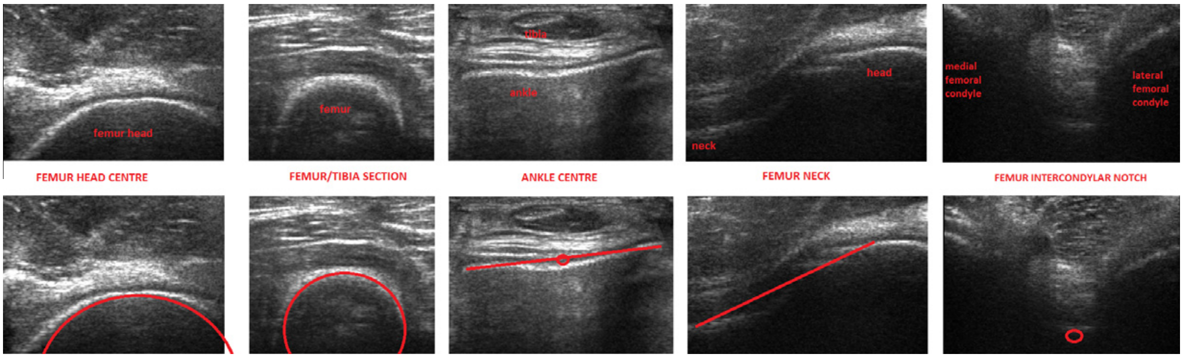


**Fig. 6.** The real ultrasonic scans of human limb (femur head, femur/tibia shaft section, ankle, femur neck and femur condyles).

*2.3.1. Comparative US and MRI tests on probands*

The five probands: 4 men and 1 woman, aged 25–33 years were examined. The courses of the mechanical axis of both lower limbs were specified basing on the ultrasound data and the data from magnetic resonance imaging. To determine the course of lower limb mechanical axis, using 3D sonography, the scans of the hip, the knee and the ankle were registered. The center of the hip was approximated as the middle point of three centers of circles fitted to the femur head echoes on three scans recorded in various intersections. The center of the knee was determined as the middle point of the condyles notch when the most ventral points of the condyles are visualized. The center of the ankle is defined as the middle point of the tibia distal contour. On the Fig. 6 the scans with placed markers defining joints centers are visualized. The subjects of the analysis were the lengths of the lower limb, the femur and the tibia [7]. The length of the femur was defined as the distance between the prescribed measure of the femoral head center and the center of the knee. The length of the tibia is the distance between the knee and the ankle center. The length of the lower limb has been designated as the distance between the center of the hip and the center of the ankle [2,3]. The neck-shaft angle was defined as the angle between the neck axis and the shaft axis designated as the vector between the centers of the circles slices fitted to the echoes of the femur shaft on its transversal scans. The characteristic points of the neck and the femoral shaft are visualized on the Fig. 6.

During the MRI-based analysis, using Mimics 11.0 from Materialise Software, the neck axis and the centers of the joints were determined. Afterwards the 3D lengths (of the femur, tibia and the lower limb), as well as the neck-shaft angle, were calculated basing on MRI-measured anthropometric points corresponding to the ultrasound measurement. The center of the femur head was approximated as the center of sphere fitted to the three dimensional shape of the bone. The knee center was defined on the coronal scan with visible eminentia intercondylaris, as the point of notch on the femur distal epiphysis. The ankle center was defined on the coronal scan with horizontal edge of epiphysis, as the middle point of this linear contour. The femur anatomical axis was defined as a three dimensional line connecting the centers of circles fitted to femur edge on the transversal scans. The neck axis was defined on the transversal scans as a 3D middle line of the neck.

*2.3.2. Test on the patients suffering from limb deformities*

The 7 patients suffering from limb deformities, and in some cases also shortening, have been examined using the free-hand sonographic system. Five measurements have been performed for each limb of a patient.

To analyse the deformity of the limb the following parameters have been measured:

1. The lower limb length – to analyze the difference in length of limbs.
2. The thigh and shank anatomical axes – to analyse the thigh–shank angle.
3. The knee articular gap axis – to analyse LDFA (lateral distal femoral angle) and MPTA (medial proximal tibial angle) typically defined in frontal plane projection (on the X-ray).

The lower limb length was measured similarly as for probands (described in Section 2.3.1). The thigh and shank anatomical axes were measured basing on four scans for each bone. On the two proximal and the two distal scans, the centers of circles, fitted to the bone echoes on transversal scans, were defined. For each pair a middle point was calculated. The obtained two points were the two endings of the anatomical axis. The thigh–shank angle is the angle between the anatomical axes of the thigh and the shank.

There were recorded two scans, one on the medial and one on the lateral side of the knee articular gap, to define the axis of the articular gap. The axis is the line connecting the middle segments between the femur and the tibia edge (see Fig. 7). The angle between the anatomical axis of the femur and the axis of the articular gap is the LDFA. The angle between the anatomical axis of the tibia and the axis of the articular gap is the MPTA.

The results of the measurements have been described in Section 3 in Table 1.

*2.3.3. Test on the patients who undergo osteosynthesis applying Ilizarov External Fixator*

The three patients, who undergo osteosynthesis applying Ilizarov External Fixator, were examined using the developed ultrasound free-hand system. The patients were

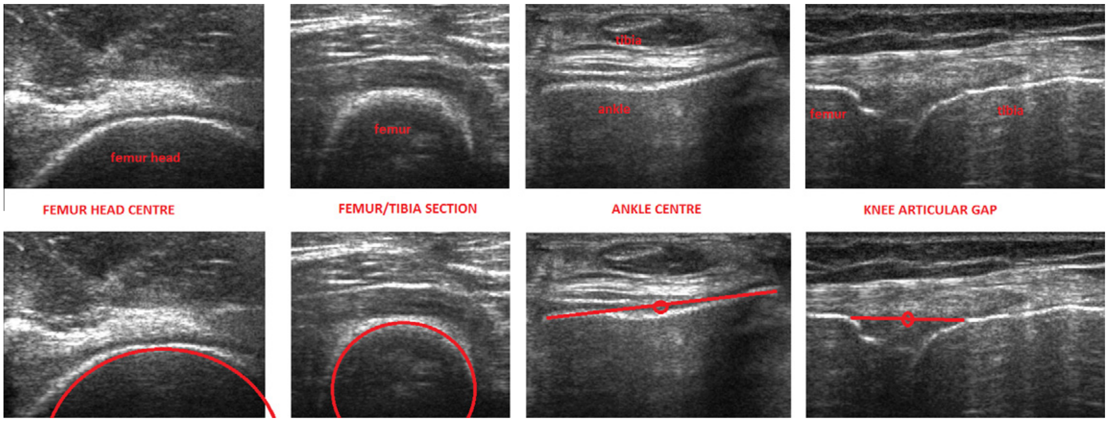


**Fig. 7.** The recorded ultrasound scans of the lower limb.

**Table 1**
The results of measurement for two patients experiencing the limb deformity.

| Parameter | Patient 1 | | Patient 2 | |
|---|---|---|---|---|
| | Right limb | Left limb | Right limb | Left limb |
| Length of mechanical axis of limb (mm) | 736.81 ± 4.36 | 710.49 ± 3.72 | 798.50 ± 3.82 | 811.69 ± 3.92 |
| Shank–thigh angle (deg) | 3.97 ± 0.97 | 15.43 ± 0.48 | 9.67 ± 1.08 | 6.02 ± 1.08 |
| LDFA (deg) | 79.28 ± 1.25 | 73.22 ± 4.01 | 79.72 ± 1.70 | 81.79 ± 1.99 |
| MPTA (deg) | 82.59 ± 0.97 | 84.03 ± 5.58 | 75.62 ± 1.18 | 80.69 ± 2.19 |
| | Patient 3 | | Patient 4 | |
| Length of mechanical axis of limb (mm) | 741.29 ± 3.48 | 741.52 ± 3.35 | 831.83 ± 4.14 | 827.45 ± 3.27 |
| Shank–thigh angle (deg) | 9.90 ± 1.15 | 13.18 ± 0.58 | 12.41 ± 1.52 | 4.39 ± 1.26 |
| LDFA (deg) | 76.79 ± 1.54 | 82.33 ± 2.25 | 78.01 ± 1.48 | 79.05 ± 1.11 |
| MPTA (deg) | 69.97 ± 0.89 | 70.81 ± 4.77 | 88.26 ± 1.95 | 78.87 ± 0.88 |
| | Patient 5 | | Patient 6 | |
| Length of mechanical axis of limb (mm) | 755.36 ± 3.17 | 729.50 ± 4.29 | 766.59 ± 4.24 | 771.96 ± 3.86 |
| Shank–thigh angle (deg) | 10.81 ± 0.68 | 12.64 ± 1.17 | 5.60 ± 0.87 | 9.93 ± 2.07 |
| LDFA (deg) | 78.43 ± 2.54 | 84.43 ± 3.37 | 79.96 ± 1.89 | 84.67 ± 2.43 |
| MPTA (deg) | 80.25 ± 2.37 | 76.21 ± 3.85 | 84.12 ± 1.79 | 82.13 ± 0.74 |
| | Patient 7 | | | |
| Length of mechanical axis of limb (mm) | 671.24 ± 4.29 | 674.91 ± 2.89 | | |
| Shank–thigh angle (deg) | 5.39 ± 2.13 | 2.25 ± 1.05 | | |
| LDFA (deg) | 82.35 ± 3.49 | 82.38 ± 2.19 | | |
| MPTA (deg) | 83.17 ± 2.51 | 84.04 ± 1.21 | | |

14–65 years old and were both slim and well-built. The tests of the same parameters as described in Section 2.3.2 section have been performed.

The results of the measurements have been described in Section 3 in Table 2.

## 3. Results

### *3.1. Results of the calibration procedure [5]*

The resulting calibration matrix using the optimization technique (method 1 in Section 2.2):

$$M_{calibration} = \begin{pmatrix} -0.926974 & 0.0131002 & -0.35332 & -54.7083 \\ -0.381023 & -0.965834 & 0.349794 & -194.651 \\ -0.248496 & 0.365218 & 0.868169 & -102.03 \\ 0 & 0 & 0 & 1 \end{pmatrix}$$

The sum of distances between the proper 3D positions of the echoes and the 3D positions of the echoes calculated using the calibration matrix equaled about 3 mm. For the single echo the minimal distance equaled 0.15 mm and the maximum distance equaled 2.4 mm.

The calibration matrix obtained using the SVD plane approximation has been estimated to:

$$M_{calibration} = \begin{pmatrix} -0.89249 & 0.23607 & -0.99905 & -60.83392 \\ -0.14107 & -0.85360 & 0.46785 & -195.44594 \\ -0.32010 & 0.41828 & -1 & -104.40520 \\ 0 & 0 & 0 & 1 \end{pmatrix}$$

The value of the summarized error was higher than 4 mm, and was strongly affected by imprecise determination of directional vectors $vx$, $vy$, $vz$ defining the rotation matrix from the phantom to the image coordinate system.

**Table 2**
The results of measurement for three patients treated with Ilizarov External Fixator.

| | Patient 8 | | Patient 9 | | Patient 10 | |
|---|---|---|---|---|---|---|
| | Left limb (with IEFon shank) | Right limb | Left limb | Right limb (with IEF on shank) | Left limb (with IEF on thigh) | Right limb |
| Length of mechanical axis of limb (mm) | 710.28 ± 2.59 | 718.35 ± 3.10 | 829.54 ± 3.87 | 809.19 ± 4.84 | 758.48 ± 4.33 | 752.00 ± 2.90 |
| Shank–thigh angle (deg) | 1.64 ± 2.21 | 23.45 ± 4.86 | 24.11 ± 2.48 | 15.90 ± 1.66 | 5.13 ± 1.81 | 6.79 ± 1.32 |
| LDFA (deg) | 87.29 ± 4.15 | 74.57 ± 4.58 | 76.18 ± 2.50 | 81.78 ± 4.79 | Not measured | Not measured |
| MPTA (deg) | 87.75 ± 3.98 | 75.19 ± 7.47 | 72.83 ± 4.06 | 80.68 ± 4.19 | Not measured | Not measured |

**Fig. 8.** The reference frame mounted on the shank distracted applying Ilizarov External Fixator.

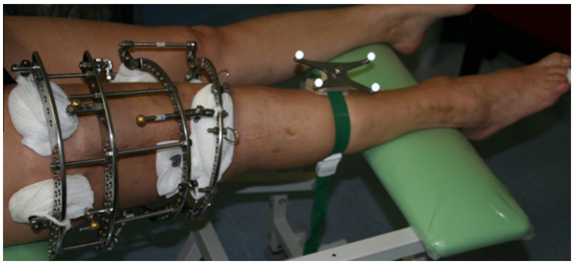

**Fig. 9.** The reference frame mounted on the shank (patient with thigh distracted applying Ilizarov External Fixator).

### 3.2. Clinical results

The ultrasound measurements were performed seven times for both legs of the probands. The repeatability expressed by the standard deviation of each measured length (femur, tibia and whole leg) range from ±1.70 mm to ±3.89 mm.

The Pearson's correlation coefficient established for the average length measured using ultrasound system and the corresponding length measured using magnetic resonance imaging was as high as 0.99. The deviations between the lengths measured by the two methods ranged from 0.42 to 4.33 mm (Fig. 10).

Also the results of the neck-shaft angle measurement using the ultrasound and the magnetic resonance imaging techniques revealed small deviations, the maximal value was as high as 2°.

Both the patients with deformities and the patients undergoing the treatment applying the Ilizarov External Fixator (IEF) on the shank and on the thigh were examined five times using the developed system (see Figs. 8 and 9). The results of the measurements on the patients suffering from deformities are presented in the Table 1, and the results obtained for the patients with IEF – are presented in the Table 2 (two patients with IEF on the shank and one with IEF on the thigh).

The presence of Ilizarov External Fixator makes the measurements more complicated. The most difficult is the measurement in the knee articular gap. Therefore the LDFA and MPTA have not been calculated for one patient with IEF on the shank (see Table 2).

The time of the first probe of complex ultrasound measurement (21 scans were recorded) in case of obese and significantly deformed patient equaled about 7 min. In case of young and thin patient the first measurement took about 3 min. The time of analysis of beforehand recorded data (i.e. identification of landmarks on scans) was always as high as 1.5 min.

## 4. Discussion

The main aim of this work was to develop the system for ultrasound noninvasive measurements of the lower limb geometry and to perform the clinical tests on probands and patients expecting the surgery and undergoing the osteosynthesis process using Ilizarov External Fixator.

The obtained accuracy of calibration is expressed as a distance between the calculated fiducial position and the position measured applying more accurate techniques. The estimated accuracy of the calibration applying the developed phantom (5 levels of double "N" structures) is comparable to the best values (range from 0.15 mm to 1.04 mm) noted by Prager et al. [13] and Mercier et al. [12]. The novelty in the proposed phantom is the higher number of fiducials and the specific double "N" structures geometry. The influence of the temperature on the speed of sound has been diminished using the temperature stabilization with the accuracy of 0.1°. The substantial factor impacting on the calibration result is the blurred, difficult to interpret, echo. This problem concerns especially the deeply located echoes with a diminished contrast. Lindseth confirms that even the automatic identification does not improve the results of calibration [10]. The most important factor by recording the image for calibration procedure is the proper focus setting to obtain optimal contrast for each fiducial echo.

The ultrasound measurements described in the paper, have been performed by the skilful US operator. The learn-

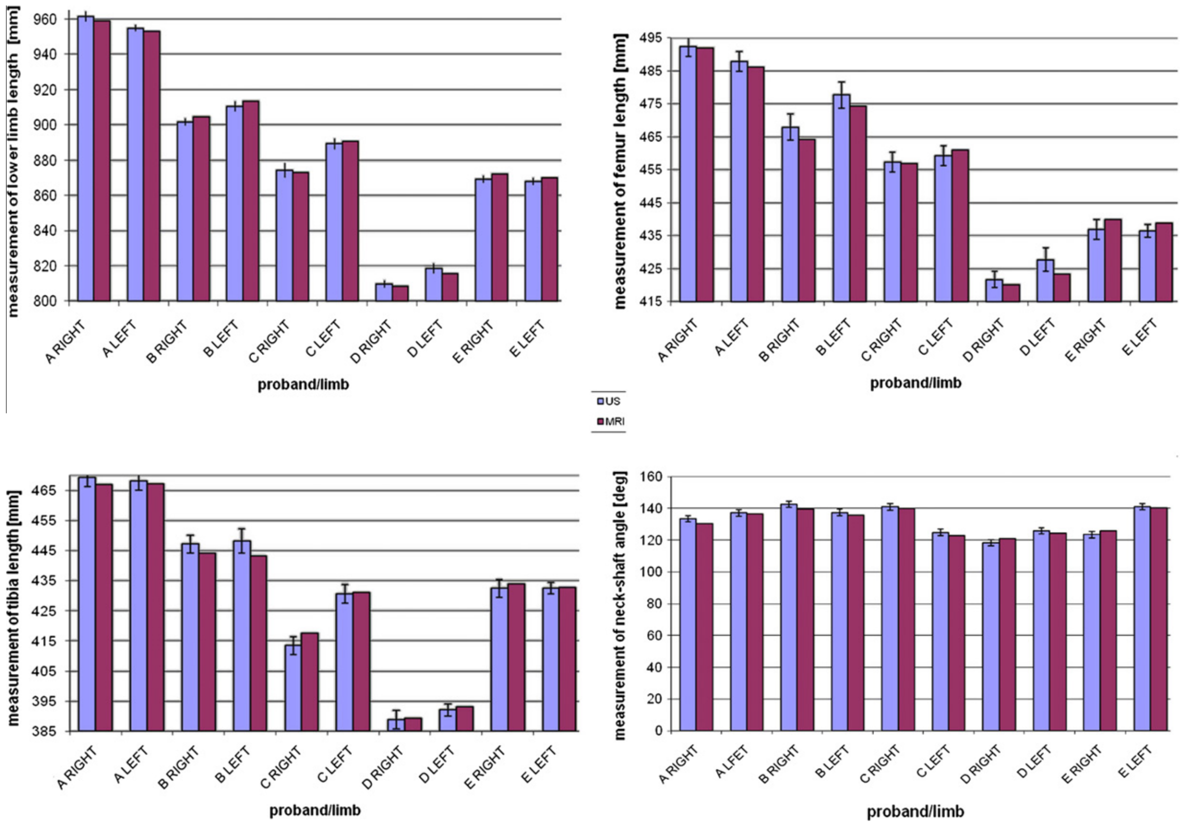


**Fig. 10.** The results of the lower limb, femur and the tibia length measurements applying 3D sonography and magnetic resonance imaging.

ing curve was typically hyperbolically shaped, nevertheless the time of measurement considerably depended on the patient obesity and existing limb deformity. Although the time of measurement seems to be considerably high, the complex procedure of measurement is performed only preoperatively, so it does not affect the time of the surgery at all. To apply the preoperatively registered data in the intraoperative conditions, the surgeon needs to register only a certain number of points to match the preoperative and the intra-operative dataset. Therefore the time of the registration does not affect the time of surgery.

The main achievement of this work is that the developed free-hand 3d ultrasound system provides high accuracy and repeatability of measurements. It has been confirmed by high correlation of the obtained results to the MRI study. It proves that the free-hand sonography can be considered as a useful tool in the clinical practice.

The limited number of examined patients using both MRI and US measurement is caused by relatively high costs and long time of examination in case of whole-leg scanning using magnetic resonance imaging. The clinical tests on a group of patients using ultrasound were repeated to check the repeatability. The tests will be continued to provide full statistical analysis, however basing on the group of 15 patients, it may be stated that the navigated ultrasound probe can be applied to analyze lower limb geometry both in physiological and pathological conditions, during and after the treatment.

The system is easily applied by a surgeon experienced in ultrasound imaging to measure the geometry of tissues, plan the surgery in the virtual reality and aid the real surgery, and finally to control the post-operative results. The system enables the surgeon to identify the bone surface on the ultrasound scans, and to reconstruct its 3D shape. The virtual surgical procedure is saved and applied intraoperatively.

The tests of system proved its usefulness in bone corrections and other orthopedic surgical procedures. The measurement on patients treated with IEF are more complicated, because of the reflections of infrared light from external fixator metallic surface and also the difficult access to the scanning region. However it has been proven, that the standard deviation in case of this group of patients, is close to the value obtained in case of probands or patients with deformities. The clinical tests proved that the developed system can be easily applied also in these conditions, as a complementary technique to the X-ray examination, to determine the three dimensional shape of bone, diagnose its deformity, design and support the surgery.

## Acknowledgement

A part of measurements has been performed applying equipment shared by Aesculap BBraun (Tuttlingen, Germany), courtesy of Professor Josef Kozak.

## References


[1] A. Fenster, K. Surry, W. Smith, D. Downey, The use of three-dimensional ultrasound imaging in breast biopsy and prostate therapy, Measurement 36 (3–4) (2004) 245–256.

[2] P. Keppler, Ch. Bartl, J. Kozak, M. Kraus, F. Gebhard, A new 2.5D ultrasound system integrated in the Orthopilot navigation system, in: Frank Langlotz, Brian L. Davies, Paul A. Grutzner (Eds.), 7th Annual Meeting of CAOS-International Proceedings (Heidelberg, Germany, June 20–23, 2007), Pro Business, Berlin, 2007.

[3] P. Keppler, W. Strecker, L. Kinzl, M. Simmnacher, L. Claes, Die sonographische bestimmung der beingeometrie, Orthopäde 28 (1999) 1015–1022.

[4] H. Kiefer, Ultrasound based versus pointer palpation method in THA Navigation – A comparative pilot study, in: 7th Annual Meeting of CAOS-International Proceedings, Heidelberg, Germany, June 20–23, 2007/red. Frank Langlotz, Brian L. Davies, Paul A. Grutzner, Pro Business, Berlin, 2007, pp. 67–69.

[5] J. Kozak, Navigation in computer-assisted surgery: comparison of navigation supported by ultrasound images with other technics of medical navigation. The works of the Institute of Biocybernetics and Biomedical Engineering, Warsaw, 2009, pp. 73.

[6] K. Krysztoforski, R. Będzinski, E. Świątek-Najwer, P. Krowicki, Calibration of free hand ultrasound probe tracked by optical system, in: R.M. Natal Jorge, Joao Manuel R.S. Tavares, Marcos Pinotti Barbosa, Alan Peter Slade (Eds.), Technology and Medical Sciences, CRC Press, Taylor and Francis Group, 2011.

[7] K. Krysztoforski, P. Krowicki, E. Swiątek-Najwer, R. Będziński, P. Keppler, Noninvasive ultrasonic measuring system for bone geometry examination, The International Journal of Medical Robotics and Computer Assisted Surgery 7 (1) (2011) 85–95.

[8] A. Kurjak, S. Kupesic, Clinical Application of 3D sonography, Parthenon Publishing, New York, 2000.

[9] P.A. Lewin, Quo vadis medical ultrasound?, Ultrasonics 42 (1–9) (2004) 1–7

[10] F. Lindseth, G.A. Tangen, T. Langø, J.B. Sintef, Probe calibration for freehand 3-D ultrasound, Ultrasound in Medicine and Biology 29 (11) (2003) 1607–1623.

[11] D. Mainard, S. Valentin, L. Galois, J. Gasnier, B. Mollard, Ultrasounds registration of the anterior pelvic plane (APP): comparison with X-ray and OrthoPilot palpation measurements, in: 7th Annual Meeting of CAOS-International Proceedings, Heidelberg, Germany, June 20–23, 2007/red. Frank Langlotz, Brian L. Davies, Paul A. Grutzner, Pro Business, Berlin, 2007, pp. 580–581.

[12] L. Mercier, T. Lango, F. Lindsesth, D.L. Collins, A review of calibration techniques for freehand 3-D ultrasound systems, Ultrasound in Medicine and Biology 31 (4) (2005) 449–471.

[13] R.W. Prager, A. Gee, G. Treece, L. Berman, Freehand 3D ultrasound without voxels: volume measurement and visualisation using the Stradx system, Ultrasonics 40 (1–8) (2002) 109–115.

[14] I.A. Rasmussen, F. Lindseth, O.M. Rygh, E.M. Berntsen, T. Selbekk, J. Xu, T.A. Nagelhus Hernes, E. Harg, A. Haberg, G. Unsgaard, Functional neuronavigation combined with intra-operative 3D ultrasound: initial experiences during surgical resections close to eloquent brain areas and future directions in automatic brain shift compensation of preoperative data, Acta Neurochirurgica 149 (4) (2007) 365–378.

[15] E. Świątek-Najwer, R. Będziński, P. Krowicki, K. Krysztoforski, P. Keppler, J. Kozak, Improving surgical precision – application of navigation system in orthopedic surgery, Acta of Bioengineering and Biomechanics 10 (4) (2008) 55–62.

[16] R. Weller, T. Pfau, M. Ferrari, R. Griffith, T. Bradford, A. Wilson, The determination of muscle volume with a freehand 3D ultrasonography system, Ultrasound in Medicine and Biology 33 (3) (2007) 402–407.